Semiconductor Physics, Quantum Electronics & Optoelectronics, 2021. V. 24, No 2. P. 166-174.

Optics

Characterization of second-order bands in Raman scattering spectra of lead phthalocyanine thin films

M.P. Gorishnyi, O.M. Fesenko

Institute of Physics, National Academy of Sciences of Ukraine
46, prospect Nauky, 03680 Kyiv, Ukraine; e-mail: miron.gorishny@gmail.com

Abstract. The structure, optical absorption (500…950 nm) and resonance Raman spectra (within the range 100…3000 cm^{-1}) of lead phthalocyanine (PbPc) thin solid films with the thickness 190 nm were studied. The films were deposited using thermal evaporation in vacuum 6.5 mPa onto silica substrates held at room temperature. It was found that in the process of depositing the PbPc thin solid films monoclinic and triclinic PbPc crystallites were grown, and the amount of crystallites in the triclinic phase in the as-deposited PbPc films was approximately two times less than those in the monoclinic one. The resonance Raman spectroscopy, with application of the He-Ne laser line 632.8 nm as an excitation source, was used for studying the 190-nm thick PbPc films. Due to resonance enhancement, the second-order Raman spectrum of PbPc films within the region 1700…2950 cm^{-1} was successfully registered and analyzed for the first time. It has been shown that the second-order PbPc Raman spectrum is mainly formed by the overtones and combination modes of B_1 symmetry fundamental vibrations. The second-order Raman region of 2550…2900 cm^{-1} appeared to be highly specific for PbPc and could be used for its identification along with the finger-print region of fundamental vibrational modes.

Keywords: thin film, optical absorption spectra, resonance Raman scattering.

https://doi.org/10.15407/spqeo24.02.166
PACS 33.20.Tp, 78.30.-j, 78.40.-q, 78.40.Me

Manuscript received 17.12.20; revised version received 26.02.21; accepted for publication 02.06.21; published online 16.06.21.

1. Introduction

The lead phthalocyanine (PbPc) molecule (Fig. 1 [1]) consists of four isoindole moieties (a benzo-fused pyrrole) that form a macrocycle phthalocyanine ligand (Pc) by using four nitrogen atoms (N=) of the azo groups. Four nitrogen atoms of the pyrrole rings form an almost square cavity, in the center of which the Pb atom is placed. This atom is located equidistantly from each of the four nitrogen atoms of the pyrrole rings and forms two valence bonds with the isoindole nitrogen atoms along the diagonal of the square cavity (Fig. 1a). The Pb atom is shifted out of the ring plane, and the phthalocyanine ring itself is no longer planar, as a result of it the PbPc molecule takes the shuttlecock-shaped configuration (Fig. 1b).

The properties of metal phthalocyanines (MPc) have been intensively studied since 1980. One of the most studied representatives of this series of coordination compounds is lead phthalocyanine. PbPc is widely used as an active material for the manufacture of gas sensors [2-6], solar cells [7-9] and field-effect transistors [10-12].

The first-order Raman spectra of PbPc within the range 100…1600 cm^{-1} have been studied in detail [13-16].

The Raman bands in the high-frequency range 1700…3250 cm^{-1} of polycrystalline powders zinc (copper) phthalocyanines (ZnPc and CuPc, respectively) were identified as the second-order spectra saving the bands of CH stretching vibrations at ~3000 cm^{-1} [17]. In [18], *ab initio* DFT simulations were carried out to describe the molecular structures, molecular orbital energy gaps, atomic charges, infrared (IR) and Raman spectra of PbPc. To the best of our knowledge, the analysis of PbPc second-order Raman spectra within the range 1700…3000 cm^{-1} was not carried out so far. In our opinion, experimental studies of Raman scattering spectra of PbPc thin films within the range 1700…3000 cm^{-1} are important and relevant in terms of ascertaining the mechanisms of interaction of basic (fundamental) vibrations in a nonplanar PbPc molecule, which may have their own features as compared to planar ZnPc and CuPc molecules. In addition, some detected second-order bands within the range 1700…3000 cm^{-1} can be used as additional markers to identify the PbPc molecule.

With account of the above considerations, we investigated the resonance Raman scattering (RRS) spectra of PbPc thin films within the range 100…3000 cm^{-1} to compare the obtained results with the literature data and to make the assignment of second-orders Raman bands of PbPc within the range 1700…2950 cm^{-1} to overtones and combinations of fundamental vibrations.

2. Experimental and sample preparation methods

Polycrystalline PbPc was kindly provided by Prof. C. Hamann from the Higher Technical School (Chemnitz, Germany). The powdery sample of PbPc was purified using extraction from solution and afterwards repeated vacuum sublimation. The impurity content in PbPc prepared in this manner did not exceed 1% [7].

The thin PbPc films with the thickness close to 190 nm were deposited using thermal evaporation in vacuum 6.5 mPa on silica substrates kept at room temperature. The mass of PbPc loaded into the ceramic crucible was 13 mg. The thickness of films was controlled with an interference thickness gauge MII-4.

UV-vis absorption spectra within the range 500…950 nm were recorded using the Perkin Elmer Lambda 25 UV-vis spectrophotometer with a spectral width of 1 nm at room temperature. The absorbance and wavelength measurements error did not exceed 2%.

The RRS spectra of PbPc films were measured using the inVia Renishaw confocal Raman microscope (England). A He-Ne laser with the wavelength λ = 632.8 nm was used as the excitation source. The light scattered and reflected by the samples passed through a Rayleigh filter, and its Raman component was decomposed into a spectrum by a diffraction grating spectrograph and focused on a CCD matrix. The electrical signal from the CCD was analyzed using Renishaw WIRE 3.3 software. The error in measuring the Raman shift did not exceed 1 cm^{-1}.

Surface morphology of PbPc thin films was characterized using a scanning electron microscope JSM-35 JEOL.

3. Results and discussion

3.1. Surface morphology, optical absorption and resonance Raman spectra of PbPc films

Phthalocyanines (MPc: Pc = phthalocyaninato anion $C_{32}H_{16}N_8^-$, M = H_2 or divalent metals) are compounds that have a macrocycle ring with a large π-conjugated aromatic system. The geometry of PbPc molecule is shown in Fig. 1. MPc generally have highly symmetrical square planar D_{4h} structures, however, unlike many MPc compounds, lead (II) phthalocyanine (PbPc) has a peculiar non-planar shuttlecock-shaped structure with C_{4v} symmetry [19].

The surface morphology of the vacuum deposited 190-nm thick PbPc thin solid films is shown in Fig. 2. Needle-like crystallites of different lengths are clearly seen.

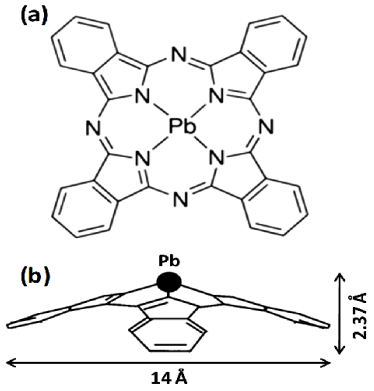

Fig. 1. The structure of the PbPc molecule: (a) top view and (b) side view [1].

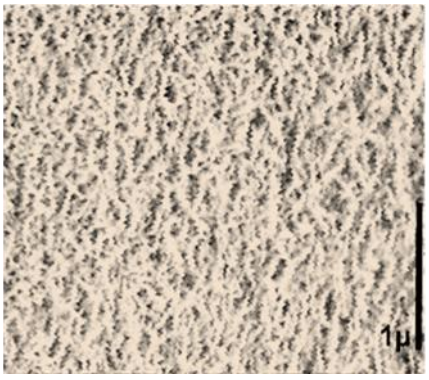

Fig. 2. SEM micro-image of the surface of 190-nm thick vacuum deposited PbPc thin solid film.

PbPc crystallizes into two modifications of monoclinic or triclinic system [19]. The electronic absorption spectra measured for the PbPc thin film have two main absorption bands. The short-wave absorption band, centered at about 350 nm, is known as the *B*-band. The longer wavelength band, centered at about 730 nm, is generally known as the *Q*-band. A fragment of the optical absorption spectrum of the PbPc films in the range of the *Q*-band (500…950 nm) is shown in Fig. 3a. Using the Origin 8.5 computer software, the overall contour of this band could be presented as the sum of three Lorentzian components with maxima centered at 657, 731 and 826 nm with the correlation coefficient and the weighted average deviation of 0.99969 and $1.0482 \cdot 10^{-4}$, respectively. The amount of monoclinic and triclinic crystalline phases in the prepared PbPc thin films can be estimated from the analysis of the peak intensities of corresponding components. It is known that for triclinic crystallites the intensity of the long-wave component at 826 nm is the highest, while the other two short-wave bands are several times weaker. For the monoclinic phase, situation is opposite and the most intensive is the band centered at 731 nm [20]. As seen from Fig. 3a, the spectral profile for the as-deposited PbPc film is similar to that expected for a monoclinic system, which shows that the vacuum deposited film consists mainly of monoclinic crystals. According to [21],

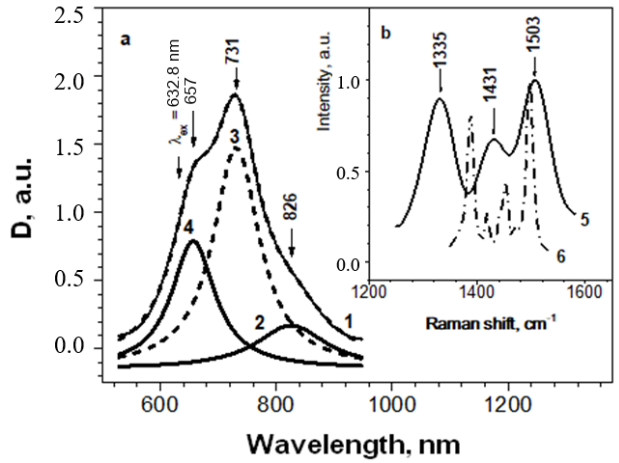

Fig. 3. Spectra of PbPc thin solid film: (*a*) optical absorption within the range of *Q*-band and (*b*) RR scattering in the fingerprint range (curve *5*). The curves *2*, *3* and *4* show the result of the *Q*-band fitting with 3 Lorentzian components, and curve *1* – the resulted band shape (dashed line) and observed band (solid line). Curve *6* corresponds to the non-resonance Raman spectra of polycrystalline powder PbPc [17].

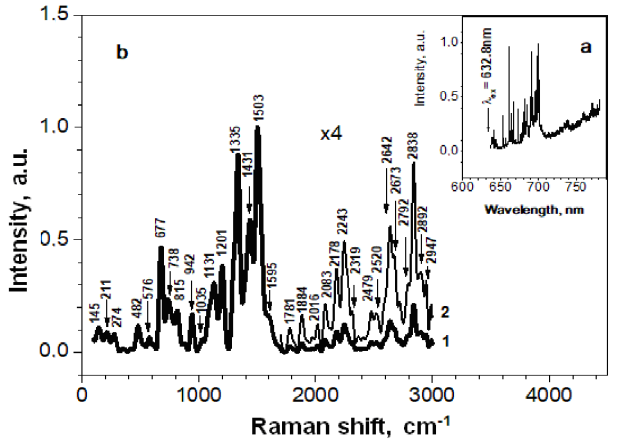

Fig. 4. Raman spectra of 190-nm thick PbPc films within the range 100…3000 cm^{-1}: (a) before and (b) after smoothing and correcting the baseline (curve *1*). Curve *2* corresponds to a fragment of the Raman spectrum of PbPc film within the range 1700…3000 cm^{-1}, magnified 4 times along the *y*-axis.

the UV-vis absorption spectra of vacuum deposited PbPc films are similar to those shown in our work (Fig. 3a). The authors of [21] also reported that after annealing the film, the changes in intensity of the absorption bands were observed, and the contour of the spectrum becomes characteristic of triclinic phase, which indicates that a monoclinic-triclinic phase transition takes place in the film [21]. It should be mentioned that the presence of these two crystal modifications in the PbPc films will not interfere with the Raman spectra since according to [17], Raman spectroscopy is not sensitive to intermolecular packing of specific phthalocyanines.

In view of the above, it can be argued that under thermal evaporation in vacuum on silica substrates held at room temperature, mainly monoclinic PbPc crystallites are present in the deposited film. In this case, the amount of triclinic crystallites in the PbPc film is about two times smaller.

The Raman scattering spectra measured in this work for the PbPc films under excitation of the He-Ne laser line 638.2 nm showed resonance enhancement and therefore should be considered as resonance Raman (RR) spectra, since the incident laser radiation (the arrow in Fig. 3a) is close in energy to the electronic transition of PbPc. In Fig. 4a, the short-wave edge of the photo-luminescence spectra of PbPc films is superimposed by the PbPc RR spectrum. The presence of this photo-luminescence emission from PbPc was confirmed in [22, 23]. Electronic excitation of a PbPc molecule results in its structural changes that are reflected in the enhancement of Raman scattering of certain vibrational modes.

Fig. 4b shows the RR spectrum of PbPc thin solid film after smoothing and baseline subtracting. The Raman shift was determined by subtracting the frequencies of the Raman spectrum ν (cm^{-1}) = $10^7/\lambda$ (nm) from the He-Ne laser frequency 15802.8 cm^{-1}. The relative intensities of the RR bands were normalized to the peak intensity of the PbPc strongest Raman band centered at 1503 cm^{-1}.

Table 1 shows the spectral parameters of the main vibration bands in the RR spectra of the 190-nm thick PbPc thin films against to the literature data for Raman spectra of other PbPc films [13, 14] and PbPc vapor phase [16].

It was found that the RR bands centered at 482, 576, 677, 738, 1131, 1201, 1335 and 1503 cm^{-1} are similar in their position to those reported by other authors [13, 14]. However, the band centered at 274 cm^{-1} was not earlier mentioned in the literature. The differences in the positions and intensities of the Raman bands reported by different authors (Table 1) are probably caused by different sample preparation methods and Raman spectra measuring techniques. We measured the RR spectra of PbPc films vacuum deposited on silica substrates without any intermediate conductive layer, while other authors used the PbPc films deposited onto conductive layers of Ag [13] or graphene [14]. The PbPc interaction with the intermediate layer may result in changes of the intensities and positions inherent to the Raman bands.

Table 2 shows spectral parameters of the first- and second-order Raman bands of PbPc thin films. In parentheses, the relative peak intensities of these bands are indicated. Table 2 also shows the positions of the first- and second-order Raman bands for polycrystalline powders CuPc and ZnPc [17]. It should be noted that the band centered at 145 cm^{-1} was earlier observed in the vapor phase of PbPc [16] and has been first

Table 1. Peak positions (in cm^{-1}) and normalized intensities (in parentheses) of main Raman bands and their assignment to molecular vibrational modes for different PbPc samples.

No	Peak position, cm^{-1}				Band assignment [13]
	RR (λ_{ex} = 632.8 nm) PbPc films on silica substrate this work	RR (λ_{ex} = 595 nm) PbPc films on Ag-coated glass substrate [13]	RR (λ_{ex} = 632.8 nm) PbPc films on graphene [14]	NR (λ_{ex} = 514.5 nm) PbPc vapor phase [16]	
	–	–	–	100	–
	–	–	–	117	–
1	145 (0.11)	–	–	149	–
	–	–	184.3	178	Macrocycle deformation
	211 (0.088)	–	205.8	216	–
	–	234, w	228.9	245	Isoindole deformation
2	274 (0.082)	–	–	–	–
3	482 (0.118)	479, m	482.7	493	Isoindole deformation
4	576 (0.066)	592, m	566.4	596	Benzene ring deformation
5	677(0.467)	672, vs	680.9	685	Macrocycle breathing
6	738 (0.234)	744, s	722.8	738	Macrocycle ring stretching
7	815 (0.185)	773, w	796.6	782	Macrocycle ring stretching
8	942 (0.170)	934, m	888.8	–	Benzene breathing
9	1035 (0.055)	1107, m	1008.2	–	C–H bend
10	1131 (0.307)	1139, m	1025.3	–	Pyrrole breathing
11	1201(0.384)	1197, w	1106.0	–	C–H bend
	–	1218, m	1193.6	–	C–H bend
	–	1303, m	1291.4	–	C–H bend
12	1335 (0.879)	1337, vs	1335.2	–	C=C pyrrole stretch
13	1431(0.589)	1423, s	1428.6	–	Isoindole ring stretch
	–	1444, w	1450.5	–	Isoindole ring stretch
	–	1484, vs	1479.3	–	C–N pyrrole stretch
14	1503 (1.000)	1505, w	1511.2	–	C–N–C azo-group stretch
15	1595(0.162)	–	–	–	Benzene ring stretch
	–	1610, w	–	–	Benzene ring stretch

Note: the bands intensities: w – weak; m – medium; s – strong; vs – very strong; NR – non-resonance Raman.

experimentally revealed in the present paper for PbPc thin films. Moreover, the first-order band centered at 482 cm^{-1} is not observed in Raman spectra of CuPc and ZnPc. In the spectra of PbPc this band is assigned to deformation vibrations of the isoindole fragment (Table 1). The absolute values of deviations in the first-order Raman frequencies of PbPc as compared to those of ZnPc are within the range 1…15 cm^{-1}, except for the bands at 274 cm^{-1}, for which these deviations are equal to 21 cm^{-1}. Deviations in the positions of the second-order Raman bands of PbPc as compared to those of ZnPc (Table 2) are in the range of 1 to 10 cm^{-1}. The bands at 2243, 2319, 2520, 2719, 2892 and 2947 cm^{-1} were not observed in either CuPc or ZnPc.

3.2. Fundamental vibrational modes of PbPc molecule

The non-planar PbPc molecule belongs to C_{4v} group symmetry and according to it molecular structure (Fig. 1) consists of $n = 57$ atoms: 8 nitrogen, 32 carbon, 16 hydrogen and one lead atoms, therefore the number of the degrees of freedom (the number of fundamental vibrational modes) of this molecule is equal to $3n - 6 = 165$. It is theoretically ascertained that distribution of these modes by different types of symmetry is as follows [18]:

$$\Gamma_{vib}=22A_1(IR,R) + 41E(IR,R) + 21B_1(R) + 21B_2(R) + 19A_2,$$

where IR and R are the vibrations active in infrared absorption and Raman spectra, respectively.

Table 2. Peak positions (in cm^{-1}) and normalized intensities (in parentheses) of major first- and second-order Raman bands for different MPc compounds: thin PbPc films and polycrystalline powders of CuPc and ZnPc.

No	First-order Raman bands, cm^{-1} (100…1700 cm^{-1})			Second-order Raman bands, cm^{-1} (1700…2950 cm^{-1})		
	PbPc film this work	CuPc [17]	ZnPc [17]	PbPc film this work	CuPc [17]	ZnPc [17]
1	145(0.11)	–	–	1781(0.027)	1788	–
2	211 (0.088)			1884(0.042)	1886	1888
3	274 (0.082)	253	253	2016(0.031)	2014	2007
4	482(0.118)	–	–	2083 (0.054)	2084	2088
5	576 (0.066)	590	587	2178(0.093)	2172	2176
6	677(0.467)	676	672	2243 (0.124)	2268	2273
7	738 (0.234)	744	743	2319(0.045)	–	–
8	815 (0.185)	830	827	2479 (0.046)	2477	2474
9	942 (0.170)	947	941	2520 (0.044)	2589	2566
10	1035 (0.055)	1034	1028	2642 (0.138)	2663	2642
11	1131 (0.307)	1122	1137	2673 (0.108)	–	–
12	1201(0.384))	1180		2719(0.056)	–	–
13	1335 (0.879)	1336	1334	2792 (0.076)	2787	–
14	1431 (0.589)	1427	1427	2838 (0.211)	–	2839
15	1503 (1.000)	1521	1501	2892 (0.088)	2860	–
16	1595 (0.162)	1587	1580	2947 (0.079)	2922	2924

Thus, Raman-active modes belong A_1, E, B_1 and B_2 symmetry types. Since the E-mode is twice degenerate, the total number of active Raman modes for the PbPc molecule is 146. The difference is 165 – 146 = 19, which coincides with the number of inactive A_2 modes.

Fig. 3b shows the RR spectra in the "fingerprints" range (1252…1581 cm^{-1}) of PbPc thin films (curve *5*) as compared to that of non-resonance Raman spectra for polycrystalline PbPc (curve *6*). As shown in [17], the 1350…1550 cm^{-1} range in the Raman spectra of metal phtalocyanines exhibits a unique pattern for each MPc, which suggests that PbPc can be identified using the vibrational bands in this area. Here, we observe three resonance Raman bands centered at 1335, 1431 and 1503 cm^{-1} for PbPc thin solid films, and the authors of [17] reported five bands in this area centered at 1388, 1418, 1453, 1470 and 1498 cm^{-1} (Fig. 3b, curves *5* and 6, respectively). The bands at 1335, 1431, and 1503 cm^{-1} are assigned to the pyrrole C=C bonds stretching vibrations, the isoindole ring breathing, and the C–N stretching vibrations of the azo groups, respectively (Table 1). The smaller number of bands in the RR spectra of PbPc films can be explained by the strong resonance enhancement and overlap of the intense bands, while the weaker bands 1418 and 1470 cm^{-1} are not seen against their background. Raman bands observed in the present paper at 1335 and 1503 cm^{-1} for PbPc films were found to be strongly shifted as compared to their position in the spectra of polycrystalline PbPc (1388 and 1498 cm^{-1}, respectively). The DFT vibrational calculations [18] predicted 14 Raman bands in the 1350…1550 cm^{-1} range (Table 1), which is useful for spectral identification of specific phthalocyanines. The difference between the RR and non-resonance Raman spectra of PbPc in the "fingerprint" region are caused by the resonance nature of the RR spectroscopy that can lead to the greatly enhanced intensity of the Raman scattering from those parts of the molecule, in which the electronic transition leads to a change in bond length or force constant in the excited state.

3.3. Overtones and combinations of fundamental vibrational modes of the PbPc molecule

When recording the RR spectrum of PbPc thin solid films by using 638.2 nm excitation, in addition to the fundamental bands we also observed first overtone and combination bands in the range 1750…2950 cm^{-1}. The intensity of these second-order Raman bands is far less than that of the first-order spectra, however, due to the resonance enhancement, the spectra are of sufficient quality for the peak positions to be obtained with good reliability. Since according to DFT vibrational calculations [18] for various MPc, including ZnPc, the major bands in their Raman spectra are assigned to the vibrations with B_1 symmetry. As reported in [17], the vibrational spectra of ZnPc and PbPc are similar in appearance, which suggests that the major bands in the Raman spectra of the PbPc solid film still belong to B_1 symmetry. Since in general the same symmetry modes are coupling, the entire first overtone and combination region can be assigned as based on the fundamental B_1 bands as well as overtones and combinations of the other fundamental bands with the same symmetry (B_2 or A_1).

Table 3. Possible assignment of the second-order Raman bands for PbPc thin solid film to overtones and combinations of fundamental modes.

No	Fundamental vibrational modes, cm^{-1}		Overtones and combinations	
			$\nu_1 + \nu_2$, cm^{-1}	ν_{exp}, cm^{-1}
	ν_1	ν_2		
1	576(0.066) (A_1)	1201 (0.384) (B_2)	1786	1781(0.027)
2	**942(0.170) (B_2)**	**942(0.170) (B_2)**	**1884**	**1884 (0.042)**
3	576(0.066) (A_1)	1431(0.589) (A_1)	2007	2016 (0.031)
4	738(0.234) (B_1)	1335(0.879) (B_1)	2073	2083(0.054)
5	738(0.234) (B_1)	1431(0.589) (B_1)	2169	2178(0.093)
6	**1131(0.307) (B_1)**	**1131(0.307) (B_1)**	**2262**	**2243(0.124)**
7	815 (0.185) (A_1)	1503 (1.000) (B_1)	2318	2319 (0.045)
8	1131(0.307) (B_1)	1335(0.879) (B_1)	2466	2479(0.046)
9	1201 (0.384) (B_2)	1335(0.879) (B_1)	2536	2520(0.044)
10	1131(0.307) (B_1)	1503 (1.000) (B_1)	2634	2642 (0.138)
11	**1335(0.879) (B_1)**	**1335(0.879) (B_1)**	**2670**	**2673 (0.108)**
12	1131(0.307) (B_1)	1595(0.162) (A_1)	2726	2719(0.056)
13	1201 (0.384) (B_2)	1595(0.162) (A_1)	2796	2792(0.076)
14	1335 (0.879) (B_1)	1503 (1.000) (B_1)	2838	2838 (0.211)
15	**1431(0.589) (A_1)**	**1431(0.589) (A_1)**	**2862**	**2892(0.088)**
16	1431(0.589) (A_1)	1503(1.000) (B_1)	2934	2947(0.079)

Table 3 shows the frequencies of the second-order Raman bands of the PbPc films within the range 1700…3000 cm^{-1}. The combinations of the main vibrational modes were selected by matching the sums of their frequencies with the corresponding frequencies of the experimentally observed PbPc Raman bands. The assignment of the main Raman bands to fundamental vibrational modes of PbPc is given in Table 1.

Because of the complicated molecular structure of PbPc molecule, most of its vibrational modes calculated in [13, 14, 16] are not a pure vibrational mode, but strongly coupled with other vibrations, and therefore the symmetry of the experimentally observed Raman bands is defined only for some of them. Moreover, there are discrepancies between the different works, so in our study we refer to the most recent DFT calculations of PbPc vibrational spectra published in [17, 18, 24]. For planar ZnPc, the position and symmetry of Raman bands within the range 200…1600 cm^{-1} were ascertained both experimentally and theoretically [18].

Comparison of the Raman spectra inherent to PbPc and ZnPc compounds shows their strong similarity in overall appearance, and so the frequencies of the corresponding fundamental vibrations of PbPc and ZnPc are not very different. Like to ZnPc, the most intense band in the PbPc spectrum (at 1503 cm^{-1}) is assigned to B_1 symmetry [17]. We assumed that the symmetry of other vibrational bands of these two compounds is also the same as presented in Table 3. The analysis of these data showed that the second-order combinations matching the second-order PbPc Raman bands are formed of fundamental vibrations of similar A_1, B_1 or B_2 symmetry.

Most of the observed second-order Raman bands can be represented as the first overtones or combinations of two fundamental vibrations of B_1 symmetry. In particular, the following first overtones and combinations of B_1 symmetry vibrations matching the experimental second-order Raman spectrum were selected (the numbers in parentheses denote the corresponding rows in Table 3): (4) 738 + 1335; (5) 738 + 1431; (6) 1131 + 1131; (8) 1131 + 1335; (10) 1131 + 1503; (11) 1335 + 1335, and (14) 1335 + 1503 cm^{-1}. Only one possible combination – the first overtone of the 942 cm^{-1} band: (2) 942 + 942 cm^{-1} could be found for fundamental vibrations with B_2 symmetry. For the fundamental vibrations of A_1 symmetry, there are only two possible combinations that match the observed second-order Raman bands: first overtone of A_1 vibration band at 1431 cm^{-1} (15) 1431 + 1431 and combination of this vibration with 576 cm^{-1} mode (3). In addition, some very weak combination bands are formed of basic vibrations with different symmetry (Table 3). In these cases, the deviation of the frequencies for the combinations of B_1 with B_2 or A_1 vibrations from those for the corresponding bands of the second order for PbPc films does not exceed ± 15 cm^{-1}.

The weak second-order band centered at 2719 cm^{-1} in Raman spectra of PbPc thin solid films, which is absent in the spectra of polycrystalline powders CuPc and ZnPc, agrees well with the combination of two fundamental vibrations of different symmetry: (12) 1131(B_1)+1595(A_1) cm^{-1} (breathing vibration of pyrrole ring and stretching vibration of benzene ring, respectively). Both modes are localized on the isoindole rings and so are easy to couple despite their different symmetry.

The intensities of the second-order Raman bands of PbPc films are approximately one–two order less than those for the fundamental bands (Fig. 4b, Table 3). This fact was also reported for polycrystalline powder CuPc and ZnPc in [17].

First overtone is a second harmonic of a fundamental vibration which is expected to prevail in the second-order vibrational spectra due to the same location in the molecular structure and the symmetry of coupling vibrations. In Table 3, the calculated frequencies of the first overtones of some fundamental vibrations of PbPc molecule are shown in bold. First overtones of the collective breathing modes of benzene and pyrroles rings, centered at 942 and 1131 cm^{-1} with the frequencies 1884 and 2262 cm^{-1}, are in good and satisfactorily agreement with the positions of the observed second-order Raman bands of PbPc films at 1884 and 2243 cm^{-1}, respectively. The second-order Raman band observed at 2673 cm^{-1} is close in its position to the first overtone of the vibrational mode 1335 cm^{-1} (stretching vibrations of the C=C bond of the pyrrole ring) with the frequency of 2670 cm^{-1}. The difference between the frequencies of the first overtone of the band at 1431 cm^{-1}, caused by the isoindole ring stretching vibration, and the second-order band at 2892 cm^{-1} of the PbPc film is 30 cm^{-1}.

The B_1 breathing mode of pyrrole rings at 1131 cm^{-1} in addition to the first overtone can form another two combinations with B_1 modes: C=C stretching of the pyrrole ring at 1335 cm^{-1} and C–N=C stretching of the azo groups at 1503 cm^{-1}, and also one combination with A_1 stretching vibration of benzene ring at 1595 cm^{-1}. The probability of these combinations is high, because the first two modes are localized on the pyrrole rings, and the benzene and pyrrole rings have common C–C and C=C bonds, and all these bands are present in the measured Raman spectra.

Thus, in our work, due to the resonance enhancement, the second-order Raman spectra of sufficient quality were measured for 190-nm thick PbPc thin solid films with the peak positions obtained with good reliability. For the first time, possible combinations of fundamental vibrational modes giving rise for the observed second-order Raman bands of PbPc thin films within the range 1700…2950 cm^{-1} have been proposed. It has been shown that the second-order PbPc Raman spectrum is mainly formed by the overtones and combination modes of B_1 fundamental vibrations. The Raman range of 2550…2900 cm^{-1} appeared to be highly specific for PbPc and could be used for its identification in composites and heterostructures along with the finger-print region of fundamental vibrational modes. This will be a subject of our further research.

4. Conclusions

It has been found that in the process of PbPc thin solid films deposition by using thermal evaporation in vacuum of 6.5 mPa on silica substrates held at room temperature, monoclinic and triclinic PbPc crystallites have been grown, and the amount of crystallites with the triclinic phase in the as-deposited PbPc films was approximately two times less.

For the first time, using the He-Ne laser line of 638.2 nm as an excitation source, the resonance Raman spectroscopy was applied for studying the 190-nm thick PbPc thin solid films. Due to resonance enhancement, the second-order Raman spectrum within the range 1700…2950 cm^{-1} has been also successfully registered and analyzed for the first time. It has been shown that the second-order PbPc Raman spectrum is mainly formed by the overtones and combination modes of B_1 fundamental vibrations. The second-order Raman range 2550…2900 cm^{-1} appeared to be highly specific for PbPc and could be used for its identification along with the finger-print range of fundamental vibrational modes.

Finally, this work has shown that resonance Raman spectroscopy can be used for characterization of the PbPc thin solid films as well as PbPc containing composite molecular systems and heterostructures.

The work was performed within the framework of the theme of the NAS of Ukraine No 14B/186.

References

1. Madhuri K.P., Sagade A.A., Santra P.K. and Tabuchi H.N.S. Templating effect of single-layer graphene supported by an insulating substrate on the molecular orientation. *Beilstein J. Nanotechnol.* 2020. **11**. P. 814–820. https://doi.org/10.3762/bjnano.11.66.
2. Mockert H., Schmeisser D., Göpel W. Lead phthalocyanine (PbPc) as a prototype organic material for gas sensors: comparative electrical and spectroscopic studies to optimize O_2 and NO_2 sensing. *Sensors and Actuators.* 1989. **19**. P. 159–176. https://doi.org/10.1016/0250-6874(89)87068-4.
3. Haman C., Kampfrath G., Mueller M. Gas and humidity sensor based on organic active thin films. *Sensors and Actuators B.* 1990. **1**. P. 142–147. https://doi.org/10.1016/0925-4005(90)80190-B.
4. Kanefusa S., Nitta M. The detection of H_2 gas by metal phthalocyanine based gas sensors. *Sensors and Actuators B.* 1992. **9**. P. 85–90. https://doi.org/10.1016/0925-4005(92)80200-H.
5. Abass A.K., Krier A., Collins R.A. The influence of iodine on the electrical properties of lead phthalocyanine (PbPc) interdigital planar gas sensors. *phys. status solidi (a).* 1994. **142**. P. 425–442. https://doi.org/10.1002/pssa.2211420216.
6. Chen J., Yu P., Zhang Y., Shan Y., Wang D. MgAl/PbPc/Cu organic thin film diode preparation and gas – sensing characteristics analysis. *Adv. Mater. Res.* 2014. **981**. P. 822–825. 10.4028/www.scientific.net/AMR.981.822.
7. Verzimacha Ya.I., Kovalchuk A.V., Kurik M.V., Haman C., Mrwa A. Solar cell of Schottky type with Ni PbPc interface. *phys. status solidi (a).* 1984. **82**. P. K111–K115. https://doi.org/10.1002/pssa.2210820165.
8. Sakurai T., Ohashi T., Kitazume H. *et al.* Structural control of organic solar cells based on nonplanar metallophthalocyanine/C60 heterojunction using

buffer layers. *Organic Electronics*. 2011. **12**. P. 966–973. https://doi.org/10.1016/j.orgel.2011.03.016.
9. Shim H.-S., Kim H.J., Kim J.W. *et al.* Enhancement of near infrared absorption with high fill factor in lead phthalocyanine based organic solar cells. *J. Mater. Chem*. 2012. **22**. P. 9077–9081. https://doi.org/10.1039/C2JM30417A.
10. Mukherjee B., Mukherjee M. Programmable memory in organic field effect transistor based on lead phthalocyanine. *Organic Electronics*. 2009. **10**. P. 1282–1287. https://doi.org/10.1016/j.orgel.2009.07.006.
11. Peng Y., Lv W., Yao B. *et al*. High performance near infrared photosensitive organic field effect transistors realized an organic hybrid planar bulk heterojunction. *Organic Electronics*. 2013. **14**. P. 1045–1051. https://doi.org/10.1016/j.orgel.2013.02.005.
12. Li Y., Zhang J., Lv W. *et al*. Substrate temperature dependent performance of near infrared photoresponsive organic field transistors based on lead phthalocyanine. *Synthetic Metals*. 2015. **205**. P. 190–194. https://doi.org/10.1016/j.synthmet.2015.04.011.
13. Jennings C., Aroca R., Hor Ah.-M., Loutfy R.O. Raman spectra of solid films – IV. Pb and Sn phthalocyanine complexes. *Spectrochim. Acta A*. 1985. **41**, No 9. P. 1095–1099. https://doi.org/10.1016/0584-8539(85)80010-6.
14. Xi L., Jin Z. Investigation of the adsorption behavior of PbPc on graphene by Raman spectroscopy. *Acta Physico-Chimica Sinica*. 2012. **28**, No 10. P. 2355–2362. https://doi.org/10.3866/PKU.WHXB201208242.
15. Dexters W., Bourgeois E., Nesladek M. *et al.* Molecular orientation of lead phthalocyanine on (100) oriented single crystal diamond surfaces. *Phys. Chem. Chem. Phys*. 2015. **17**. P. 9619–9623. https://doi.org/10.1039/C5CP00174A.
16. Voudoukis N.F. Raman spectroscopy and innovative solar cells optical characterization of molecules. *European Journal of Electrical and Computer Engineering (EJECE).* 2019. **3**, No 2. P. 1–6. https://doi.org/10.24018/ejece.2019.3.2.67.
17. Tackley D.R., Dent G., Smith W.E. Phthalocyanines: structure and vibrations. *Phys. Chem. Chem. Phys.* 2001. **3**. P. 1419–1426. https://doi.org/10.1039/B007763L.
18. Zhang Y., Zhang X., Liu Z., Xu H., Jiang J. Comparative density functional theory study of the structures and properties of metallophthalocyanines of group IVB. *Vibrational Spectroscopy*. 2006. **40**. P. 289–298. https://doi.org/10.1016/j.vibspec.2005.11.004.
19. Hamamoto N., Sonoda H., Sumimoto M. *et al.* Theoretical study on crystal polymorphism and electronic structure of lead(II) phthalocyanine using model dimers. *RSC Adv.* 2017. **7**. P. 8646–8653. https://doi.org/10.1039/C6RA27269J.
20. Collins R.A., Krier A., Abass A.K. Optical properties of lead phthalocyanine (PbPc) thin films. *Thin Solid Films*. 1993. **229**. P. 113–118. https://doi.org/10.1016/0040-6090(93)90417-N.
21. Vasseur K., Rand B.P., Cheyns D., Froyen L., Heremans P. Structural evolution of evaporated lead phthalocyanine thin films for near-infrared sensitive solar cells. *Chem. Mater*. 2011. **23**. P. 886–895. https://doi.org/10.1021/cm102329v.
22. Sharma G.D., Choudharu V.S., Roy M.S. Electrical and photovoltaic properties of devices based on PbPc TiO_2 thin films. *Solar Energy Materials and Solar Cells*. 2007. **91**, No 12. P. 1087–1096. https://doi.org/10.1016/j.solmat.2007.03.003.
23. Kalugasalam P., Ganesan S. Photoluminescence of lead phthalocyanine thin films. *Optoelectronics and Advanced Materials, Rapid Communications*. 2010. **4**, No 2. P. 154–159.
24. Tackley D.R., Dent G., Smith W.E. IR and Raman assignments for zinc phthalocyanine from DFT calculations. *Phys. Chem. Chem. Phys.* 2000. **2**. P. 3949–3955. https://doi.org/10.1039/B005091L.

Authors and CV

M.P. Gorishnyi. PhD in Physics and Mathematics, Senior Researcher of the Department of molecular photoelectronics at the Institute of Physics, NAS of Ukraine. Main directions of his scientific activity: study of optical and photoelectric properties of thin films of polyacenes, phthalocyanines and other organic compounds as well as heterostructures on their basis in order to ascertain the mechanisms of donor-acceptor interaction at the interface of heterostructures. He is the author of more than 33 publications.

O.M. Fesenko. PhD in Physics and Mathematics, Senior Researcher. The head of the Laboratory "Surface Enhanced Spectroscopy" at the Institute of Physics, NAS of Ukraine. Main areas of her researches: studying the mechanisms and effects of optical signal amplification for biological molecules located near metallic and non-metallic (carbon, metal oxide) surfaces by using IR and Raman spectroscopy, creation of new types of substrates for vibrational spectroscopy, surface-enhanced infrared absorption Raman scattering (SERS). She is the author of more than 39 publications.

Характеризація смуг другого порядку в спектрах раманівського розсіювання тонких плівок фталоціаніну свинцю

М.П. Горішний, О.М. Фесенко

Анотація. Досліджено структуру, спектри оптичного поглинання (500…950 нм) та резонансні КРС (100…3000 $см^{-1}$) тонких твердих плівок фталоціаніну свинцю (PbPc) товщиною 190 нм. Плівки осаджено термічним випаровуванням у вакуумі 6,5 мПа на витримані при кімнатній температурі кварцові підкладки. Установлено, що в процесі осадження тонких плівок PbPc виросли моноклінні та триклінні кристаліти PbPc, причому кількість кристалітів триклінної фази у свіжонанесених плівках PbPc була приблизно в два рази меншою. Для дослідження тонких твердих плівок PbPc товщиною 190 нм була застосована резонансна раманівська спектроскопія з використанням He-Ne лазерної лінії 632,8 нм як джерела збудження. Завдяки резонансному підсиленню вперше було успішно зареєстровано та проаналізовано спектр КРС плівки PbPc другого порядку в області 1700…2950 $см^{-1}$. Було показано, що спектр КРС другого порядку PbPc формується переважно з обертонів та комбінаційних мод основних коливань симетрії B_1. Спектральна ділянка 2550…2900 $см^{-1}$ спектрів КРС виявилася надзвичайно специфічною для PbPc і може бути використана для його ідентифікації разом із областю відбитків пальців основних коливальних мод.

Ключові слова: тонка плівка, оптичні спектри поглинання, резонансне раманівське розсіювання.